SUPPLEMENTARY INFORMATION

Effect of Slight Structural Changes on Gelation Properties of *N*-phenylstearamide Supramolecular Gels

Alexandre R. Meyer,[a] Caroline R. Bender,[a] Daniel M. dos Santos,[a] Francieli I. Ziembowicz,[b] Clarissa P. Frizzo,[a] Marcos A. Villetti,[b] José M. Reichert,[c] Nilo Zanatta,[a] Helio G. Bonacorso[a] and Marcos A. P. Martins[a*]

[a]*Núcleo de Química de Heterociclos (NUQUIMHE), Department of Chemistry, Federal University of Santa Maria,*[b] *Laboratório de Espectroscopia e Polímeros (LEPOL), Department of Physics,* [c]*Laboratório de Física do Solo, Soil Department, Federal Universityof Santa Maria, 97105-900, Santa Maria, RS, Brazil*

*e-mail: marcos.nuquimhe@gmail.com

Synthesis and spectral data of *N*-phenylstearamide

Stearic acid (0.34 g, 1.2 mmol), *N,N'*-Dicyclohexylcarbodiimide (0.25 g, 1.2 mmol) and 4-Dimethylaminopyridine (0.03 g, 0.25 mmol) were dissolved in dried dichloromethane (30 mL) in a round-bottom flask, equipped with a stir bar. After 30 min, the aromatic amine (1 mmol) was slowly added. The reaction mixture was stirred at 25 °C for 48 h. Afterwards, the dichloromethane was evaporated under reduced pressure. The solid obtained was recrystallized twice in ethanol furnishing the *N*-Phenylstearamides.
For characterization data, ^{1}H and ^{13}C NMR spectra, recorded on a Bruker Avance III (^{1}H at 600.13 MHz and ^{13}C at 150.903 MHz; BRUKER BioSpinGmBH, Germany) in $CDCl_3$/TMS solutions. Electrospray ionization mass spectra (ESI-MS) was performed in an Agilent Model 6460 Triple quadrupole 6460 (LC/MS-MS; Agilent Technologies, USA) operating in the positive-ion mode. The melting points were measured using a MDSC Q2000 (T-zero TM DSC technology, TA Instruments Inc., New Castle, DE, USA). The solid samples were subjected to three cycles of heating and cooling in the temperature range of 25 °C to 200 °C (at a heating rate of 5 °C min^{-1}).

N-phenylstearamide. Yield 56%, m.p. 86.8 °C. ^{1}H-NMR (600.13 MHz, $CDCl_3$, δ): 0.88 (t, 3H), 1.26 (s, 28H), 1.69-1.74 (m, 2H), 2.34 (t, 2H), 7.09 (t, 1H), 7.15 (s, 1H), 7.30 (t, 2H), 7.49 (d,2H). ^{13}C-NMR (150.903 MHz, $CDCl_3$, δ): 14.1, 22.7, 25.7, 29.3, 29.4, 29.5, 29.6, 29.7, 32.0, 37.9, 119.9, 124.2, 129.0, 138.0, 171.2; Positive ESI-MS *m/z* 360 $[M + H]^+$.

N-(4-tolyl)stearamide. Yield 64% m.p. 91.6 °C. ^{1}H-NMR (600.13 MHz, $CDCl_3$, δ): 0.88 (t, 3H), 1.25 (s, 28H), 1.70-1.72 (m, 2H), 2.30 (s, 3H), 2.33(t, 2H), 7.10 (d, 2H), 7.37

(d,2H). ^{13}C-NMR (150.903 MHz, $CDCl_3$, δ; ppm): 14.1, 20.1, 22.7, 25.7, 29.3, 29.4, 29.5, 29.6, 29.7, 32.0, 37.8, 120.0, 129.5, 133.9, 135.4, 171.5; Positive ESI-MS *m/z* 374 $[M + H]^+$.

N-(4-acetylphenyl)stearamide. Yield 69% m.p. 108.4 °C. ^{1}H-NMR (600.13 MHz, $CDCl_3$, δ): 0.88 (t, 3H), 1.26 (s, 28H), 1.69-1.77 (m, 2H), 2.37(t, 2H), 2.54 (s, 3H), 7.36 (s, 1H), 7.60 (d, 2H), 7.91 (d,2H). ^{13}C-NMR (150.903 MHz, $CDCl_3$, δ): 14.1, 22.8, 25.6, 26.4, 29.4, 29.5, 29.6, 29.7, 29.8, 32.1, 38.1, 119.2, 130.9, 133.3, 142.6, 171.7, 190.8; Positive ESI-MS *m/z* 402 $[M + H]^+$.

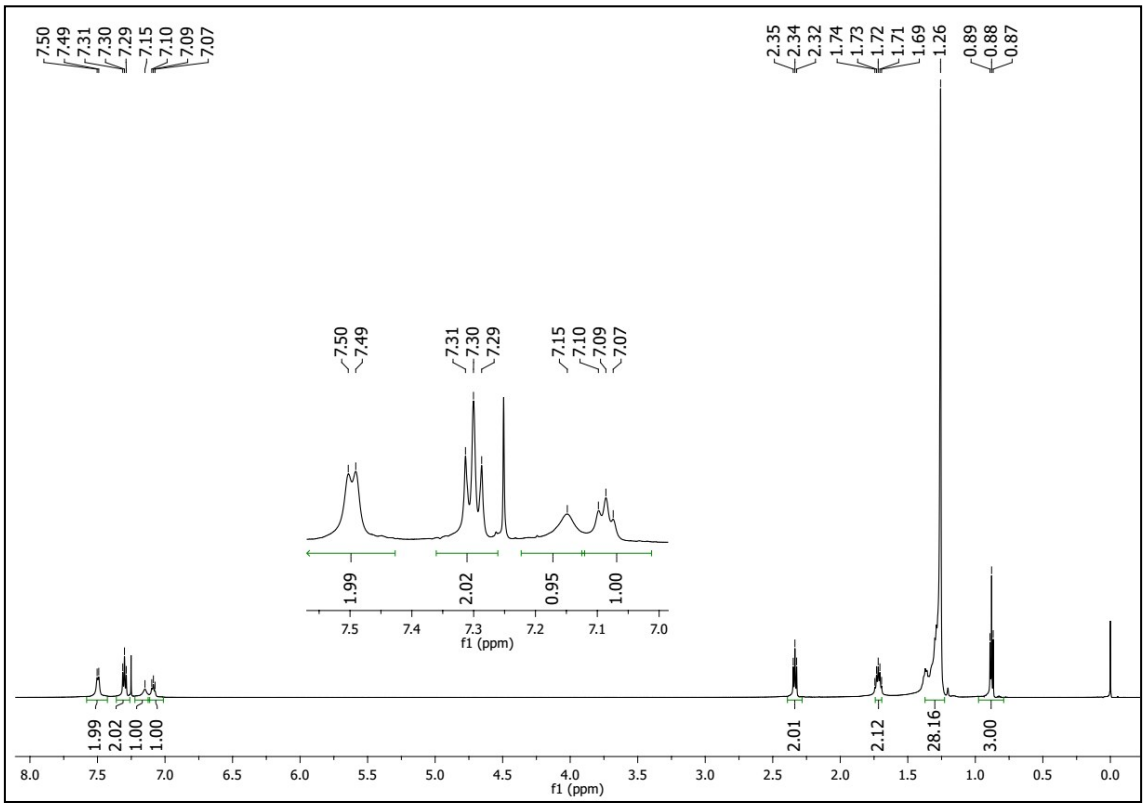

Figure S1. ^{1}H RMN spectra of compound **1** in $CDCl_3$, 600.13 MHz (40°C).

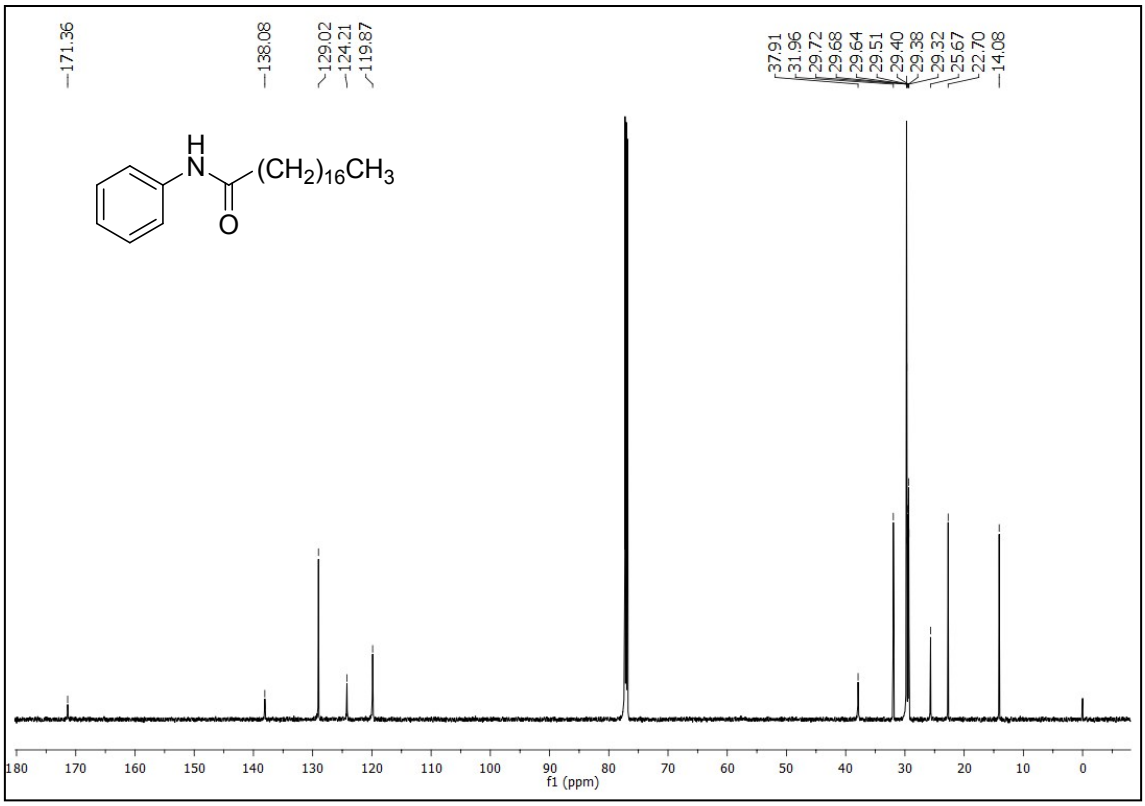

Figure S2. ^{13}C RMN spectra of compound **1** in $CDCl_3$, 150.903 MHz (40°C).

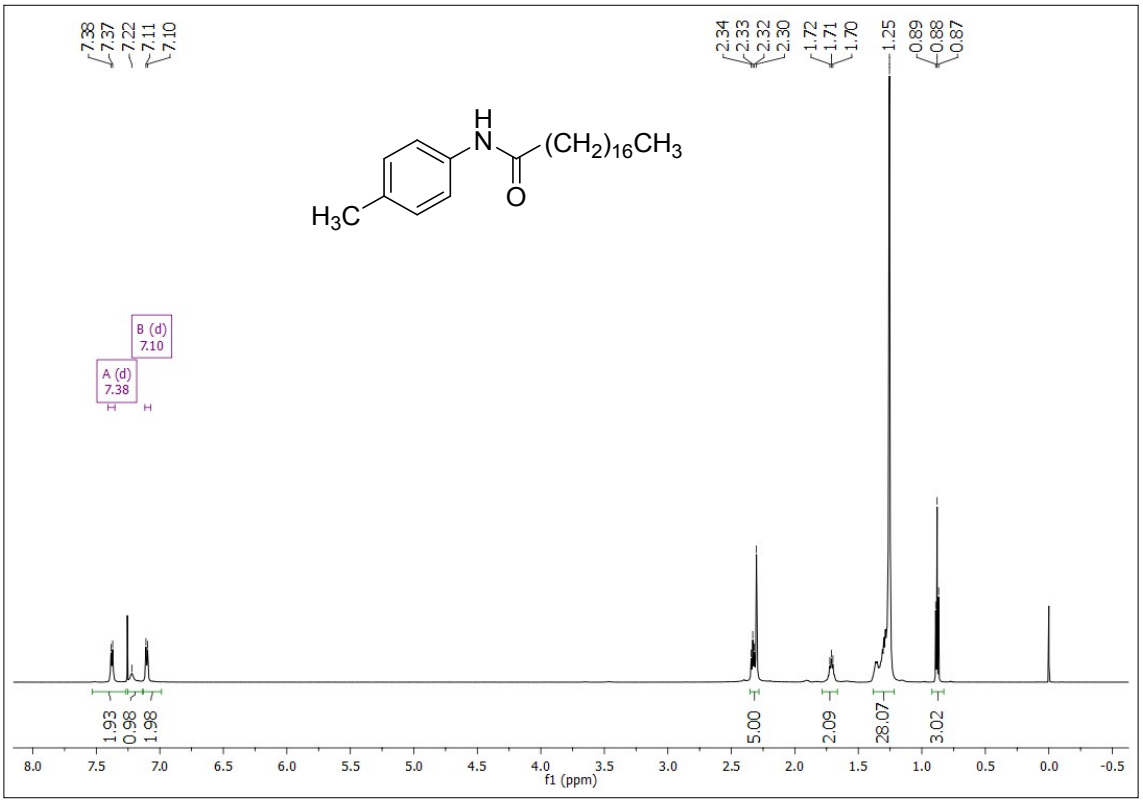

Figure S3. ^{1}H RMN spectra of compound **2** in $CDCl_3$, 600.13 MHz (40°C).

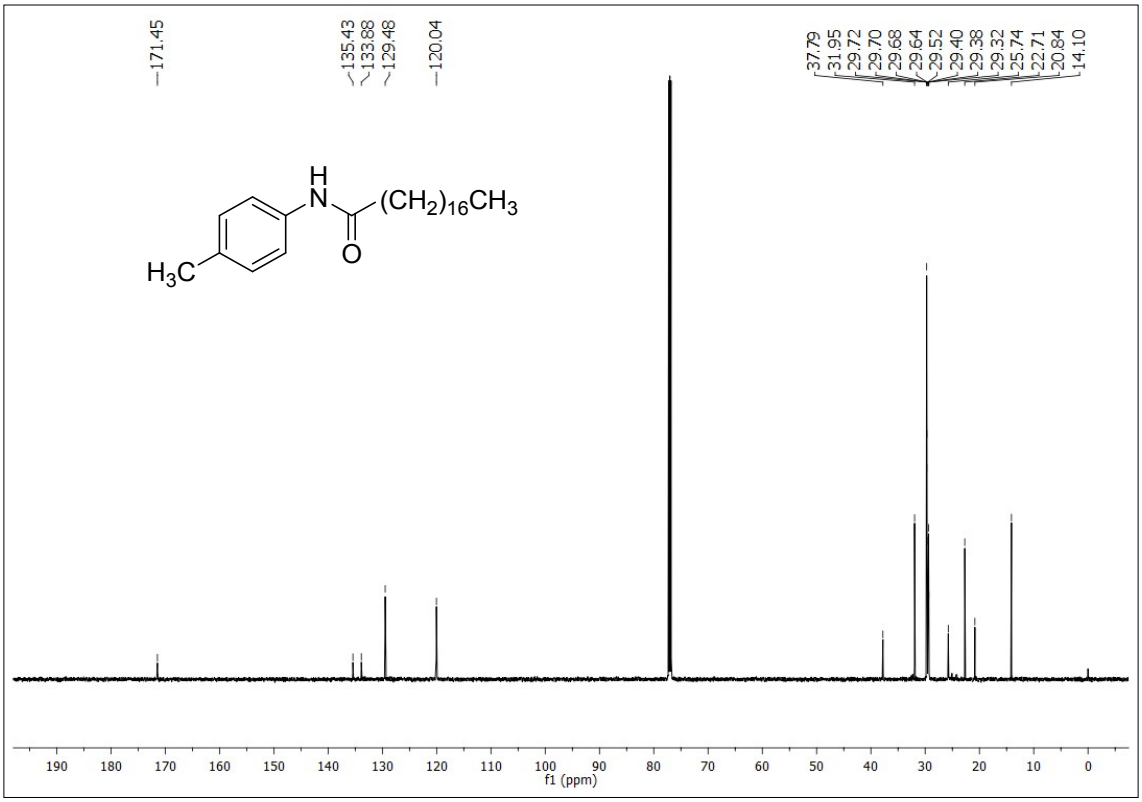

Figure S4. ^{13}C RMN spectra of compound **2** in $CDCl_3$, 150.903 MHz (40°C).

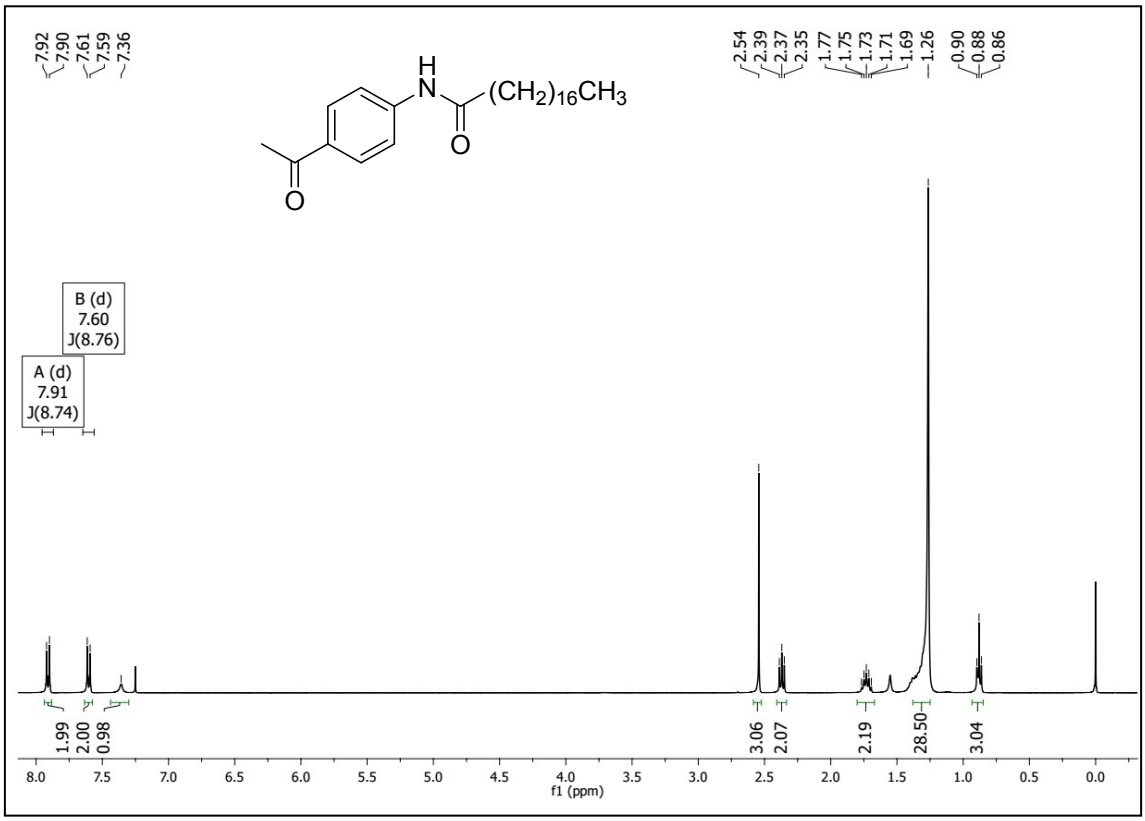

Figure S5. ^{1}H RMN spectra of compound **3** in $CDCl_3$, 600.13 MHz (40°C).

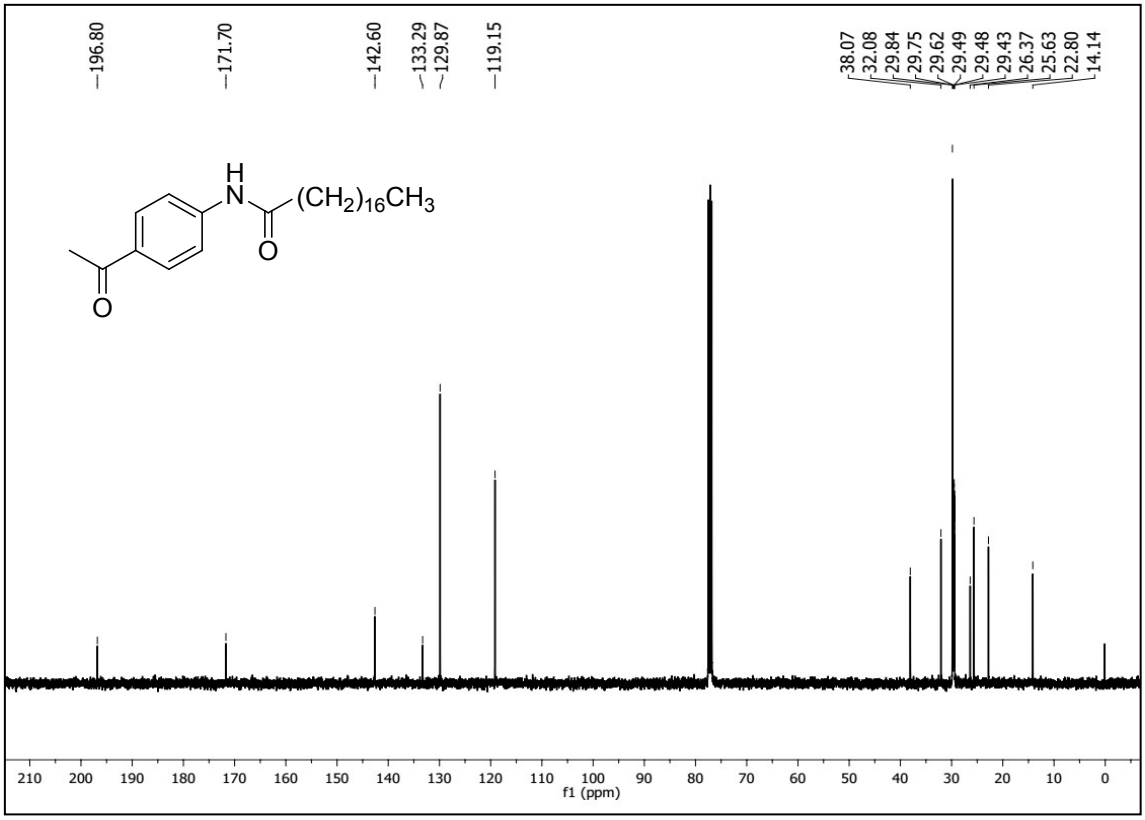

Figure S6. ^{13}C RMN spectra of compound **3** in $CDCl_3$, 150.903 MHz (40°C).

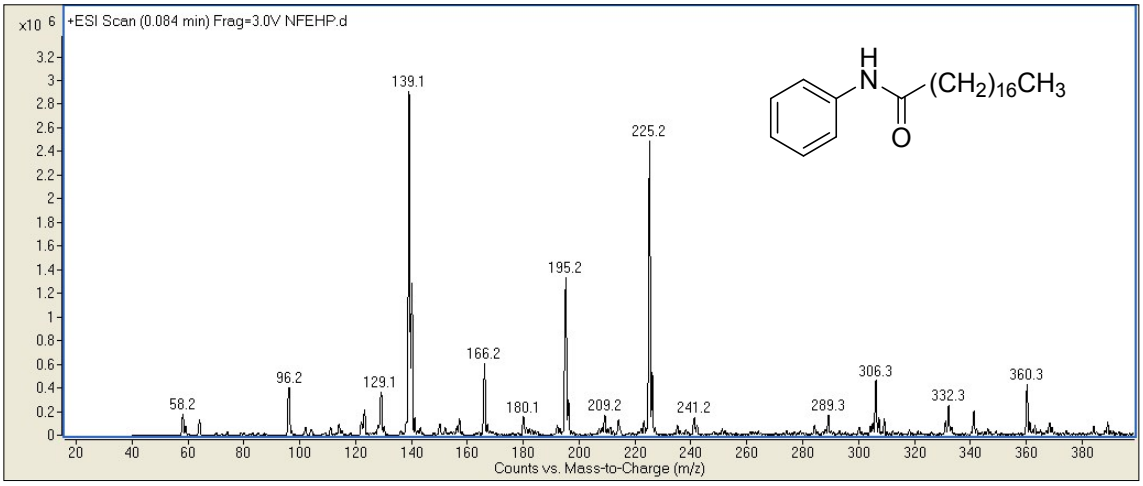

Figure S7. Mass spectra of compound **1** (LC-MS positive mode).

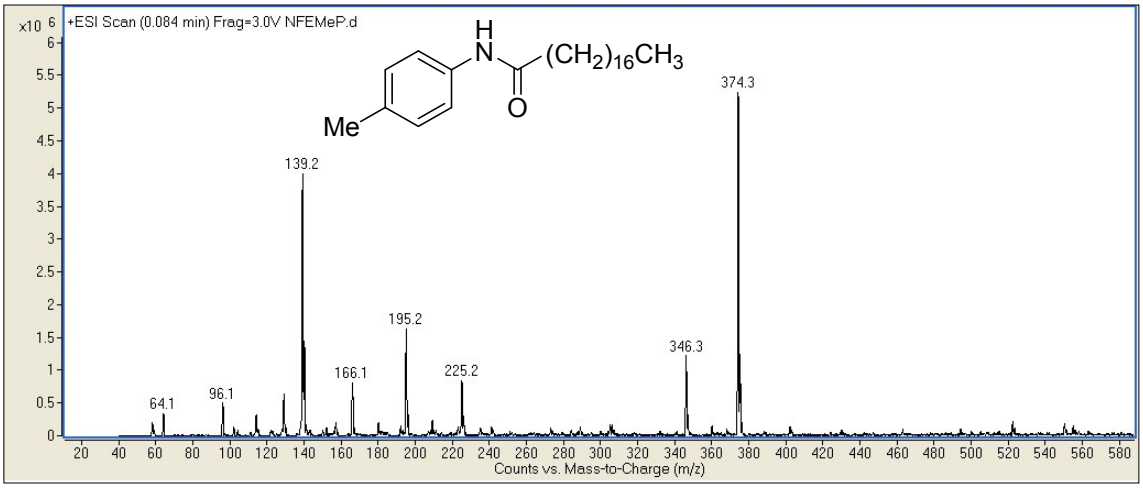

Figure S8. Mass spectra of compound **2** (LC-MS positive mode).

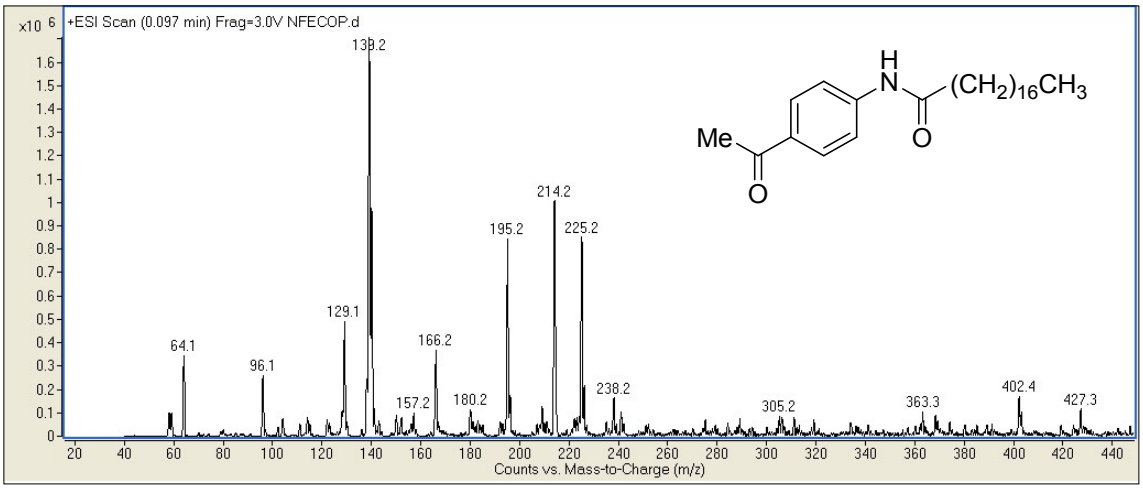

Figure S9. Mass spectra of compound **3** (LC-MS positive mode).

Gelation Behavior

a) b) c) d) e) f) g) h)

Figure S10. Supramolecular gel of compound **2** in: a) cyclohexane, b) benzene, c) toluene, d) ethyl acetate, e) acetonitrile f) ethanol, g) DMSO, h) acetone.

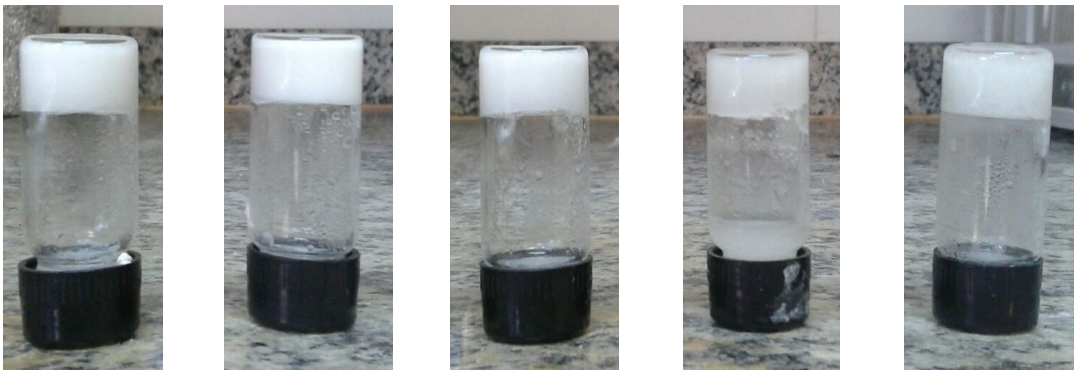

a) b) c) d) e)

Figure S11. Supramolecular gel of compound **3** in: a) cyclohexane, b) benzene, c) toluene, d) acetonitrile e) DMSO.

UV-Vis spectroscopy

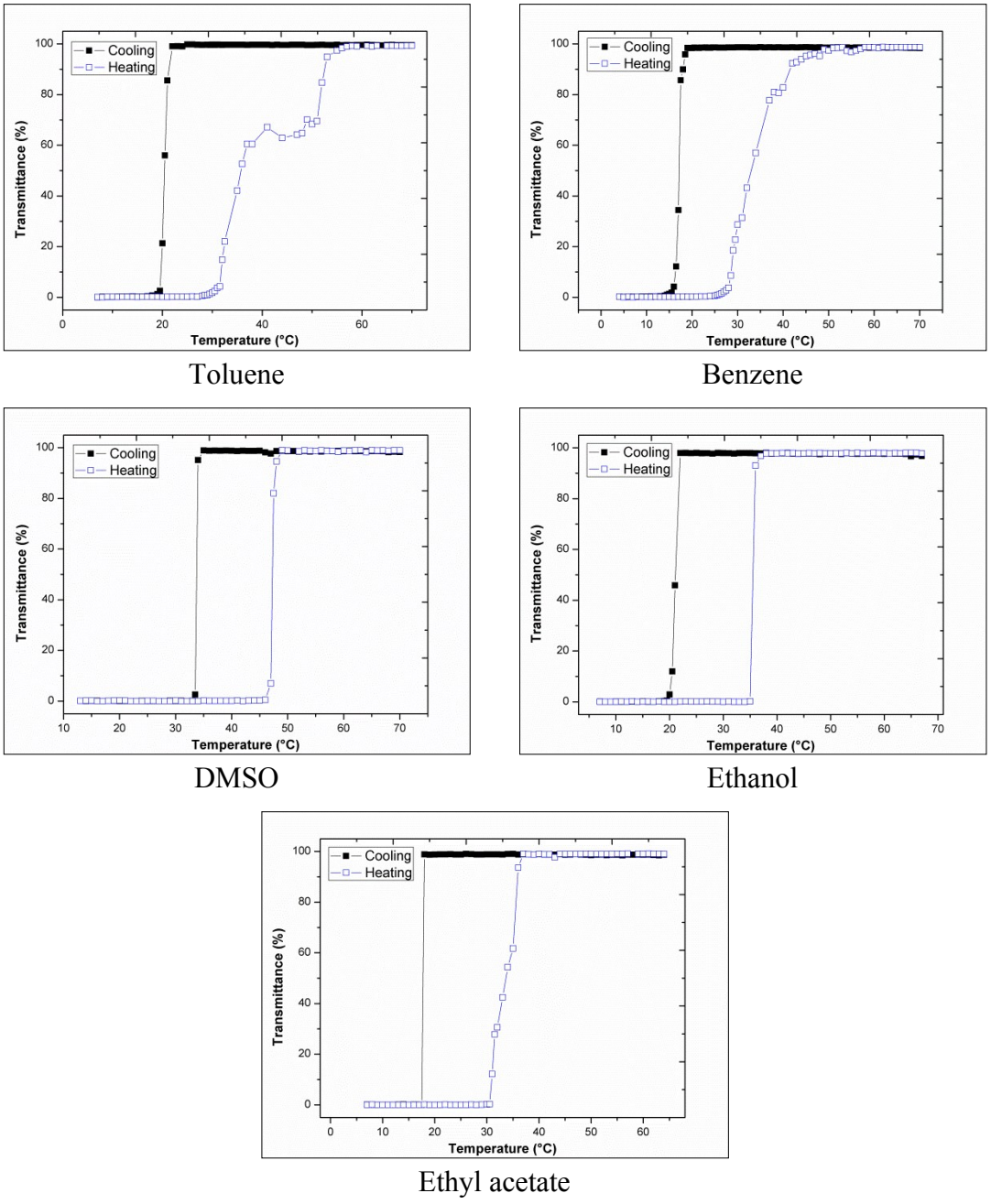

Figure S12. Transmittance *versus* temperature curves of **1** in several solvents.

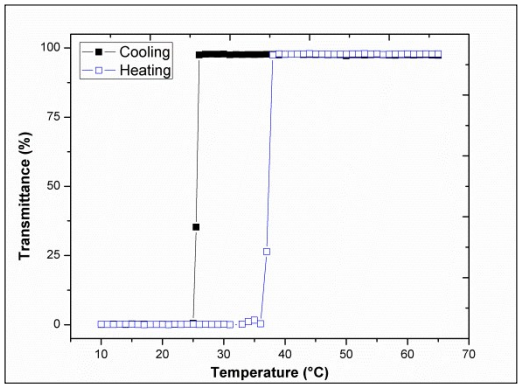

Ethyl acetate

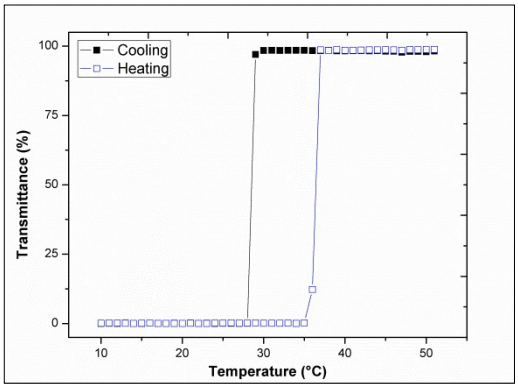

Acetone

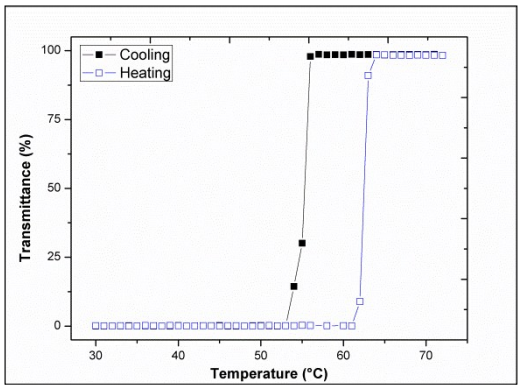

Acetonitrile

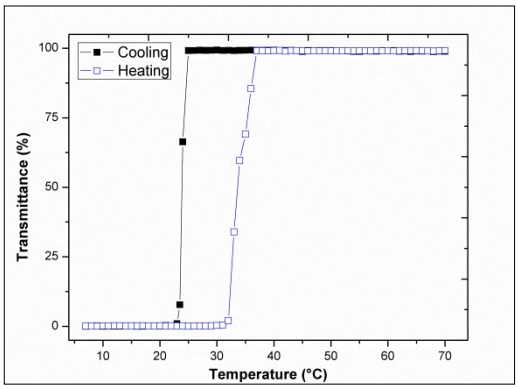

Benzene

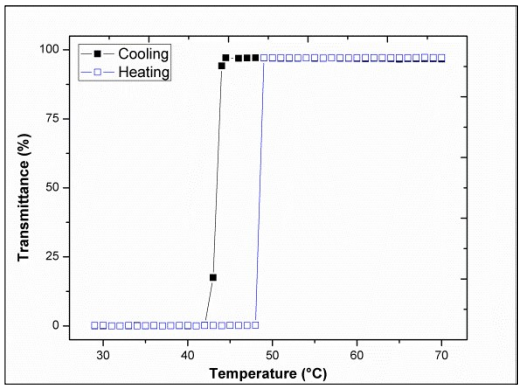

Cyclohexane

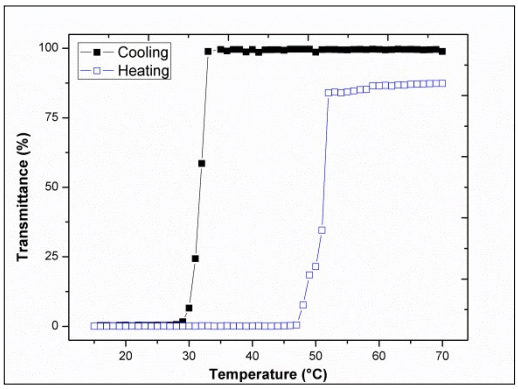

DMSO

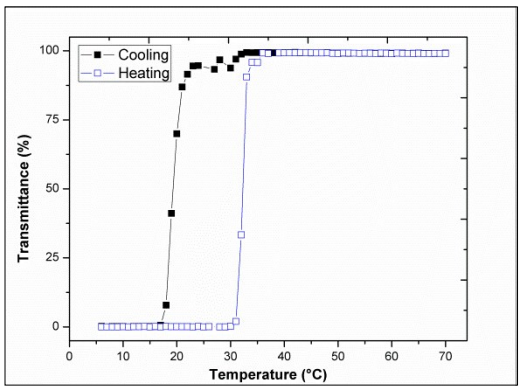

Ethanol

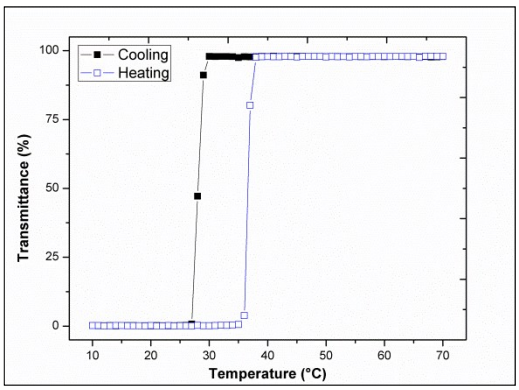

Toluene

Figure S13. Transmittance *versus* temperature curves of **2** in several solvents.

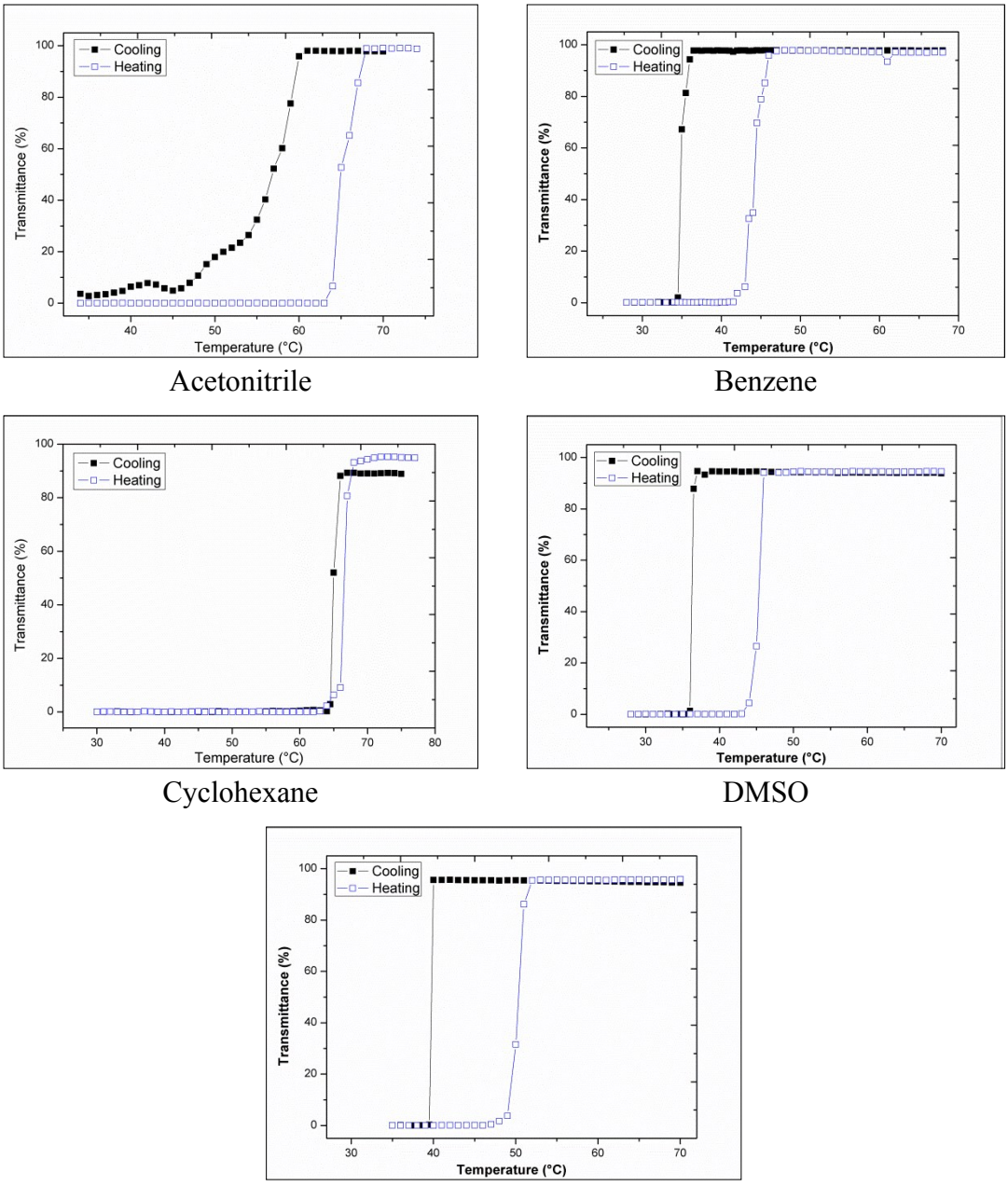

Figure S14. Transmittance *versus* temperature curves of **3** in several solvents.

DSC Curves

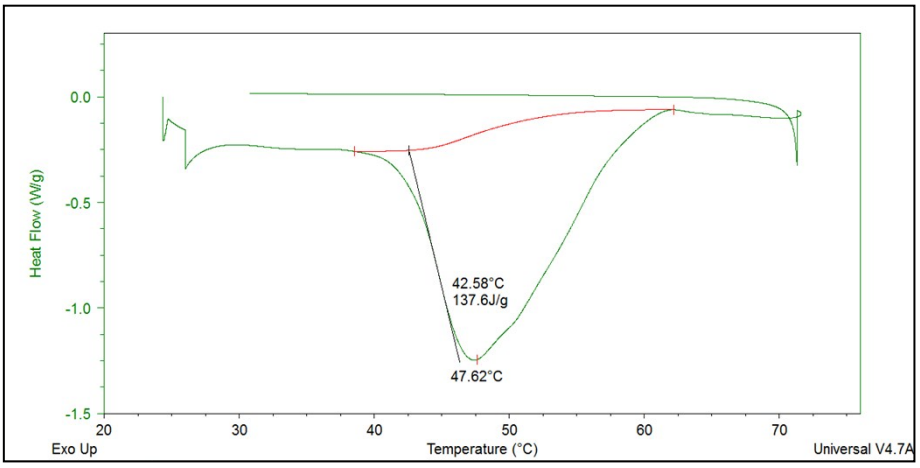

Figure S15. DSC curve of gel formed from **1** (R = H) in ethyl acetate at heating rate of 5 °C min^{-1}.

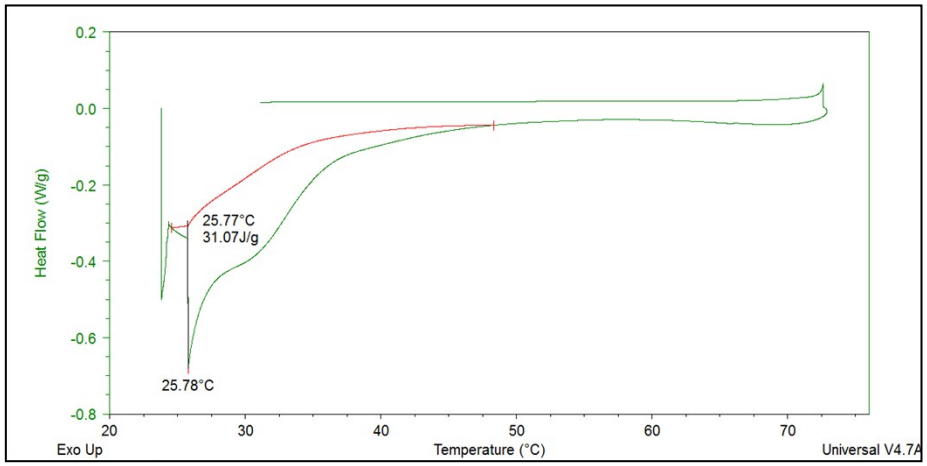

Figure S16. DSC curve of gel formed from **1** (R = H) in benzene at heating rate of 5 °C min^{-1}.

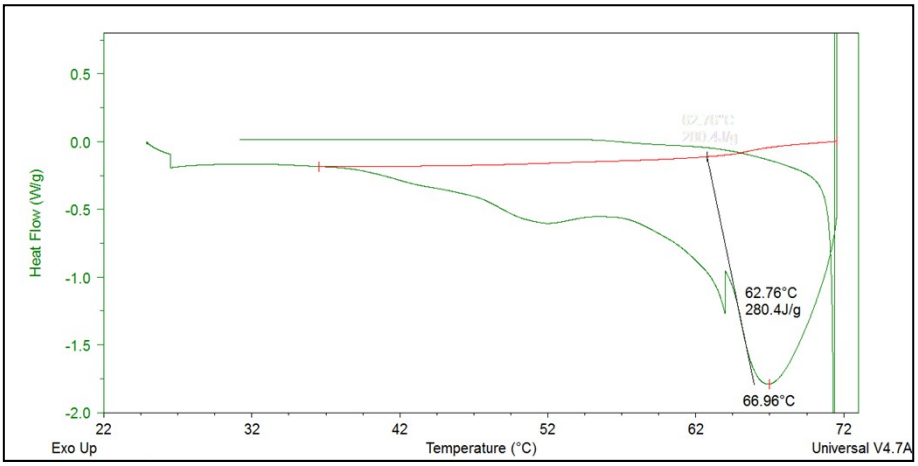

Figure S17. DSC curve of gel formed from **1** (R = H) in ciclohexane at heating rate of 5 °C min^{-1}.

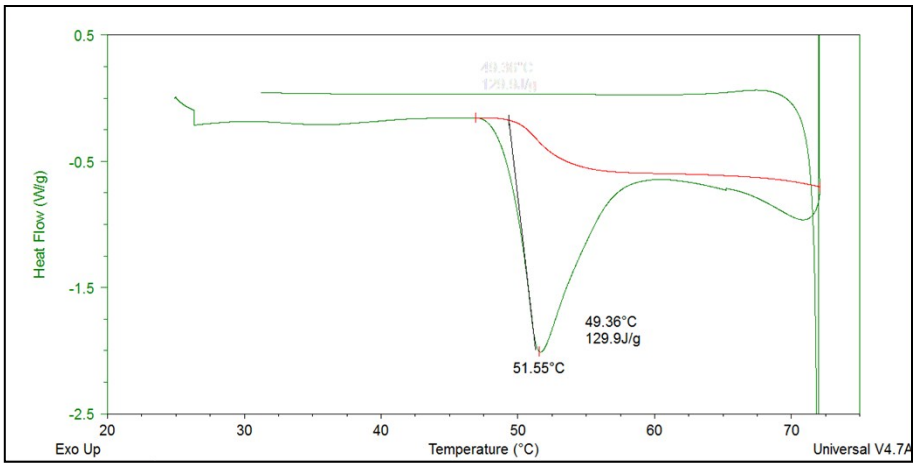

Figure S18. DSC curve of gel formed from **1** (R = H) in toluene at heating rate of 5 °C min^{-1}.

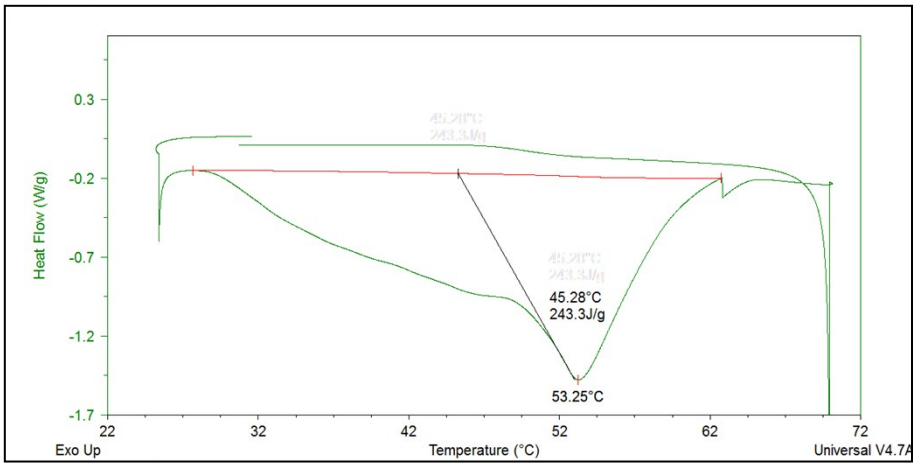

Figure S19. DSC curve of gel formed from **1** (R = H) in acetonitrile at heating rate of 5 °C min^{-1}.

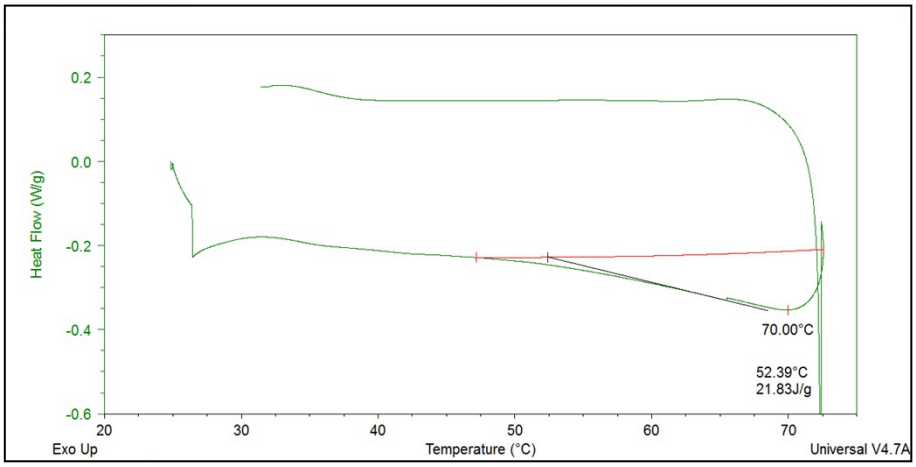

Figure S20. DSC curve of gel formed from **1** (R = H) in DMSO at heating rate of 5 °C min^{-1}.

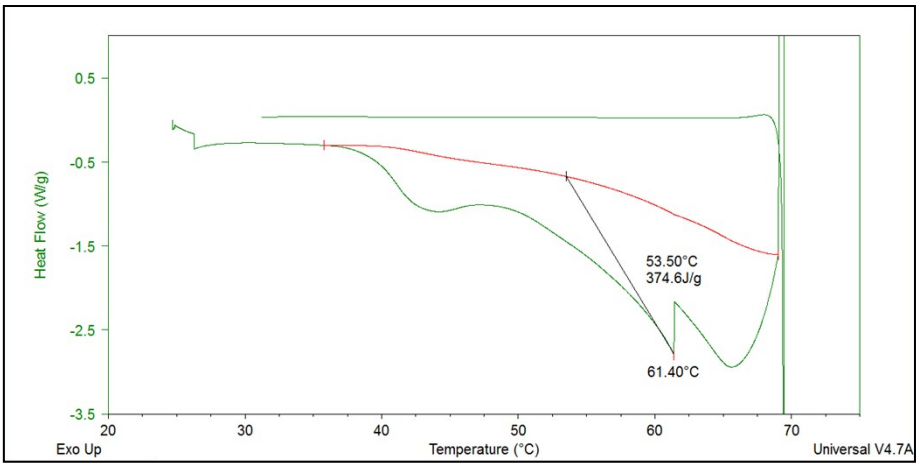

Figure S21. DSC curve of gel formed from **1** (R = H) in ethanol at heating rate of 5 °C min^{-1}.

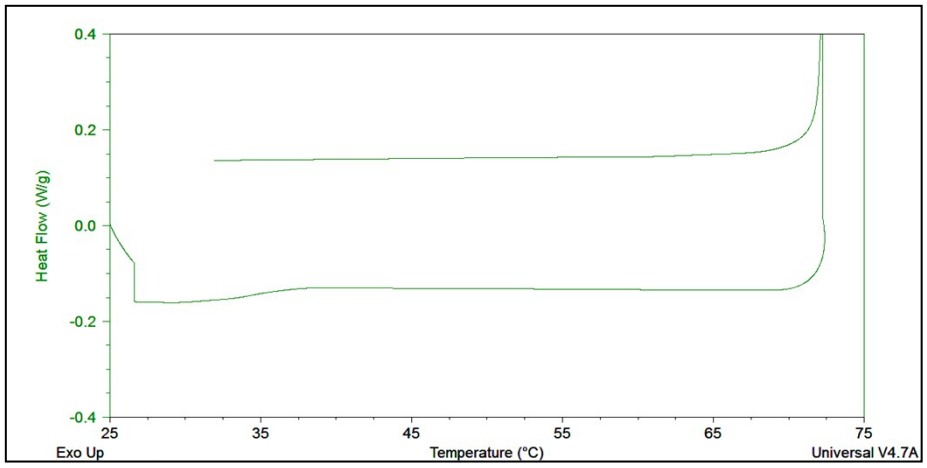

Figure S22. DSC curve of gel formed from **2** (R = CH_3) in benzene at heating rate of 5 °C min^{-1}.

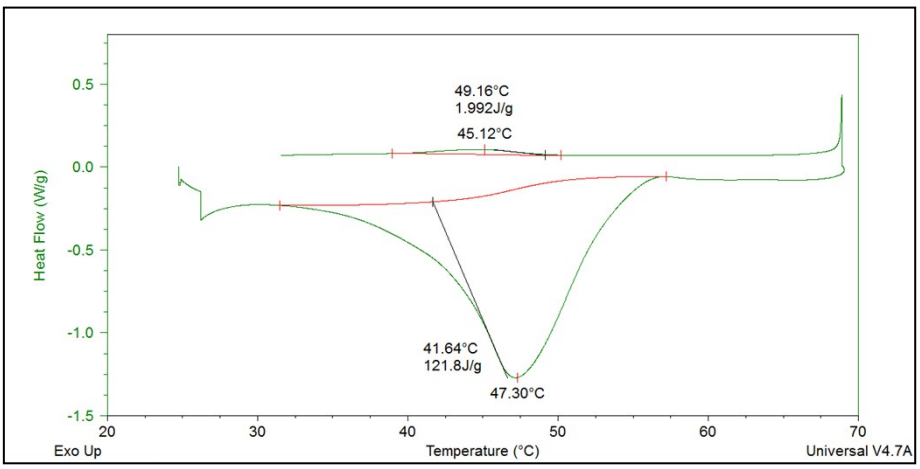

Figure S23. DSC curve of gel formed from **2** (R = CH_3) in ethyl acetate at heating rate of 5 °C min^{-1}.

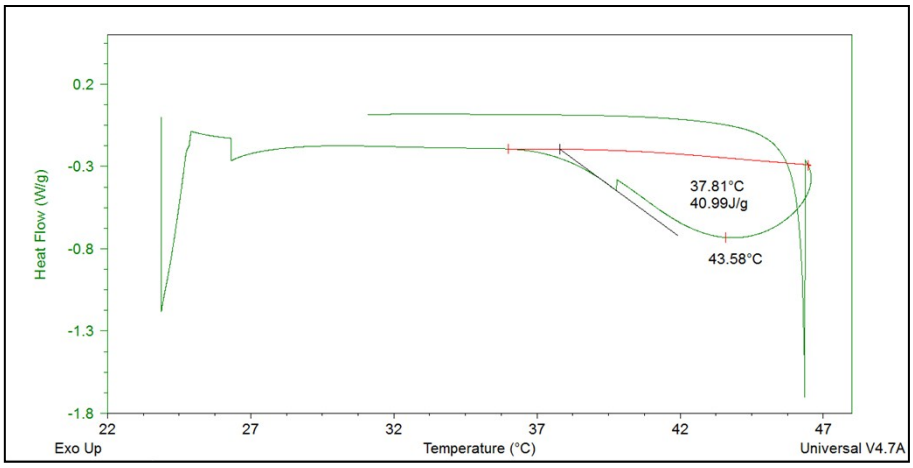

Figure S24. DSC curve of gel formed from **2** (R = CH_3) in acetone at heating rate of 5 °C min^{-1}.

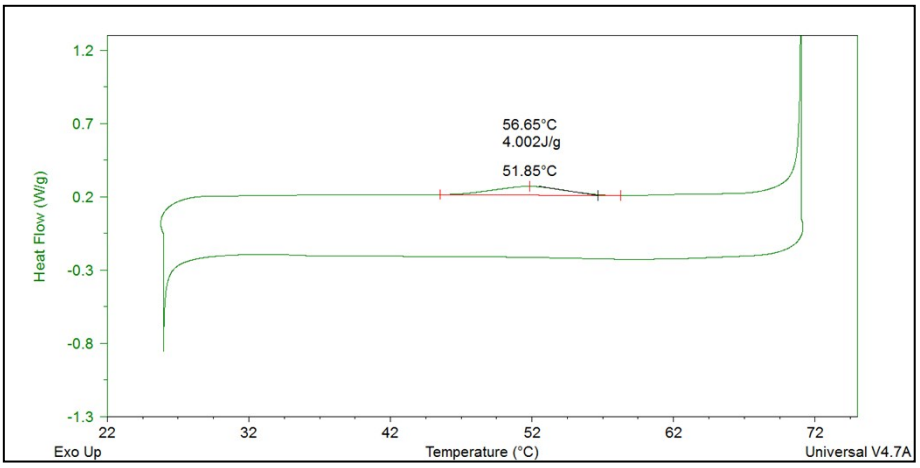

Figure S25. DSC curve of gel formed from **2** (R = CH_3) in acetonitrile at heating rate of 5 °C min^{-1}.

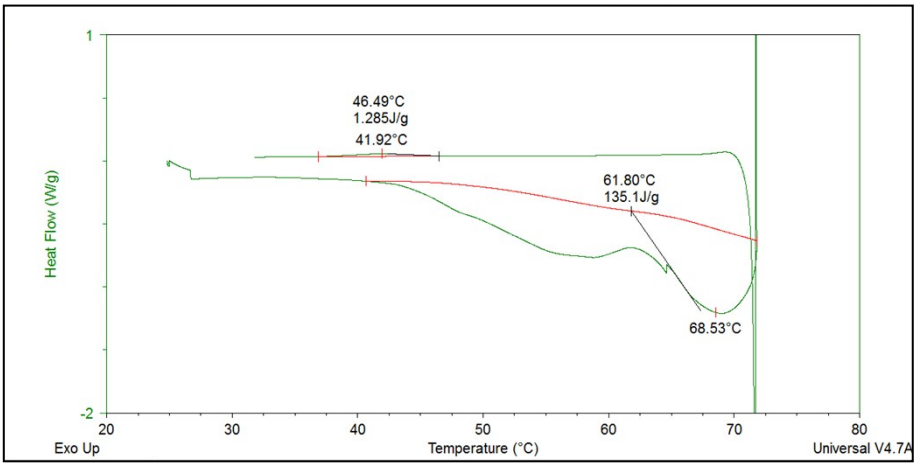

Figure S26. DSC curve of gel formed from **2** (R = CH_3) in ciclohexane at heating rate of 5 °C min^{-1}.

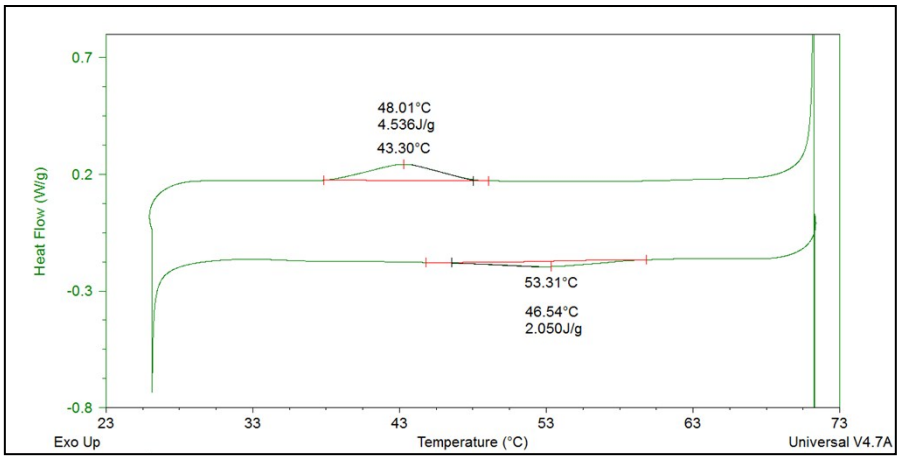

Figure S27. DSC curve of gel formed from **2** (R = CH_3) in DMSO at heating rate of 5 °C min^{-1}.

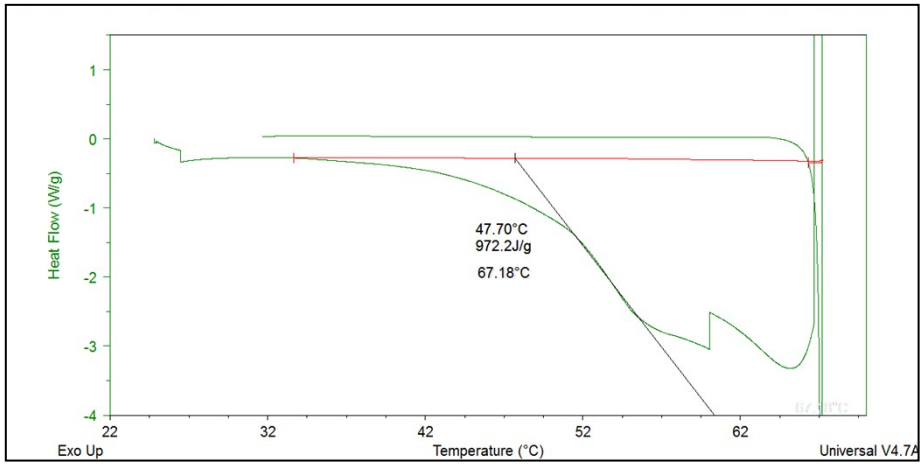

Figure S28. DSC curve of gel formed from **2** (R = CH_3) in ethanol at heating rate of 5 °C min^{-1}.

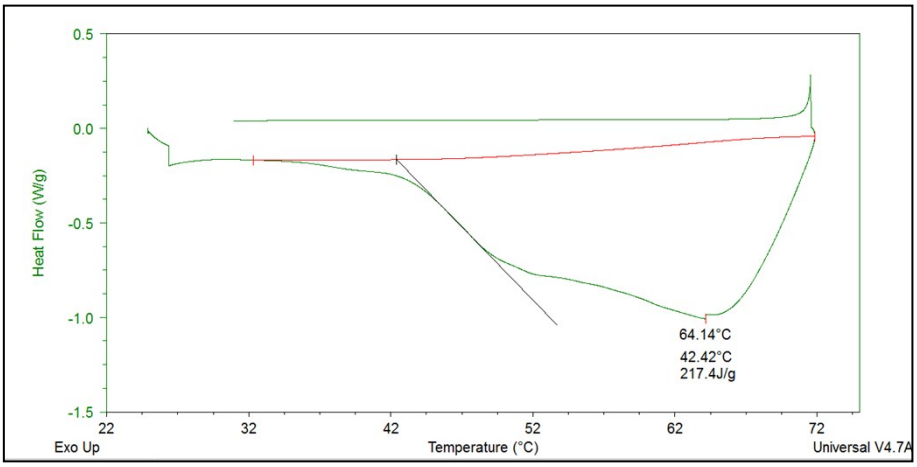

Figure S29. DSC curve of gel formed from **2** (R = CH_3) in toluene at heating rate of 5 °C min^{-1}.

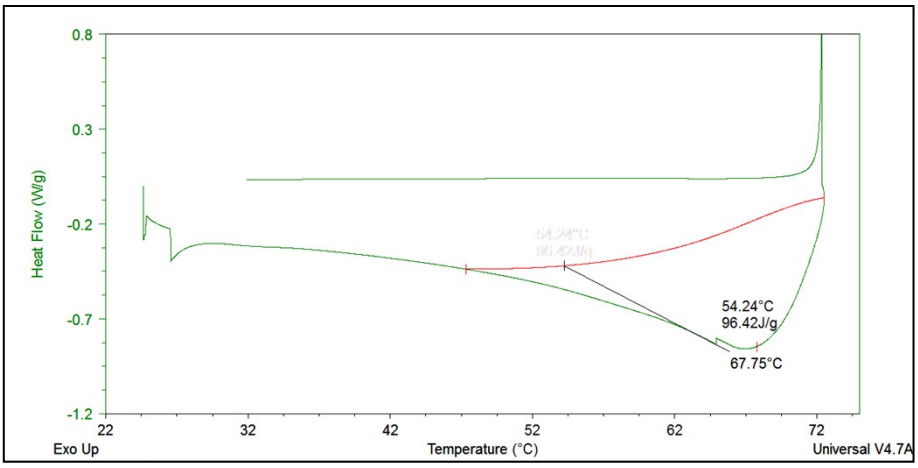

Figure S30. DSC curve of gel formed from **3** (R = $COCH_3$) in acetonitrile at heating rate of 5 °C min^{-1}.

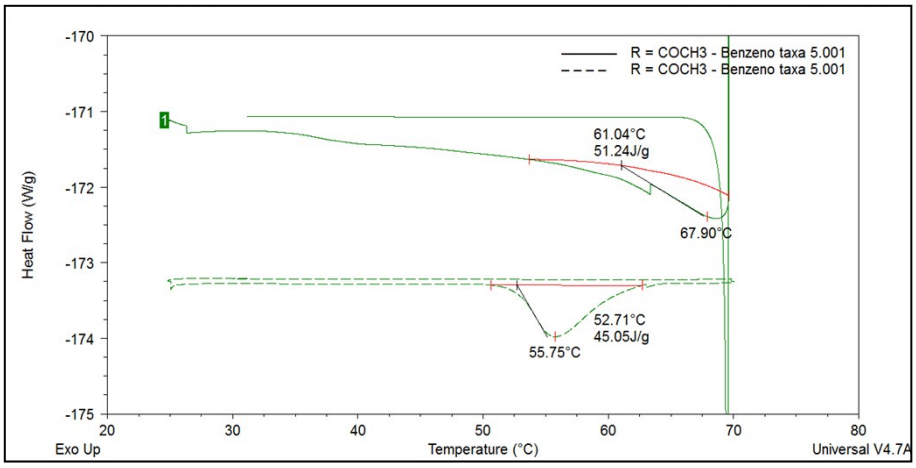

Figure S31. DSC curve of gel formed from **3** (R = $COCH_3$) in benzene at heating rate of 5 °C min^{-1}.

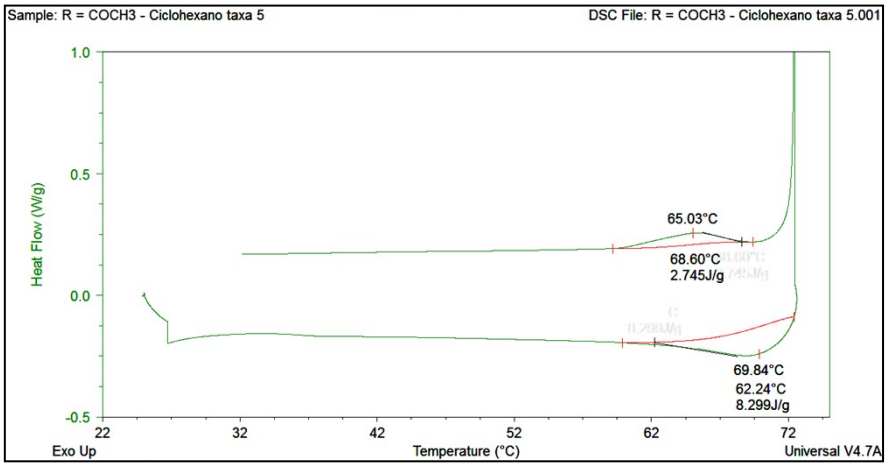

Figure S32. DSC curve of gel formed from **3** (R = $COCH_3$) in ciclohexane at heating rate of 5 °C min^{-1}.

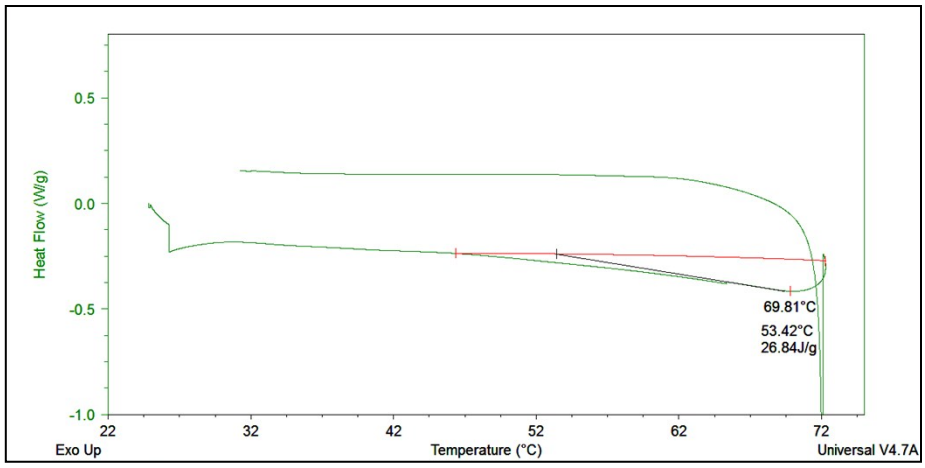

Figure S33. DSC curve of gel formed from **3** (R = $COCH_3$) in DMSO at heating rate of 5 °C min^{-1}.

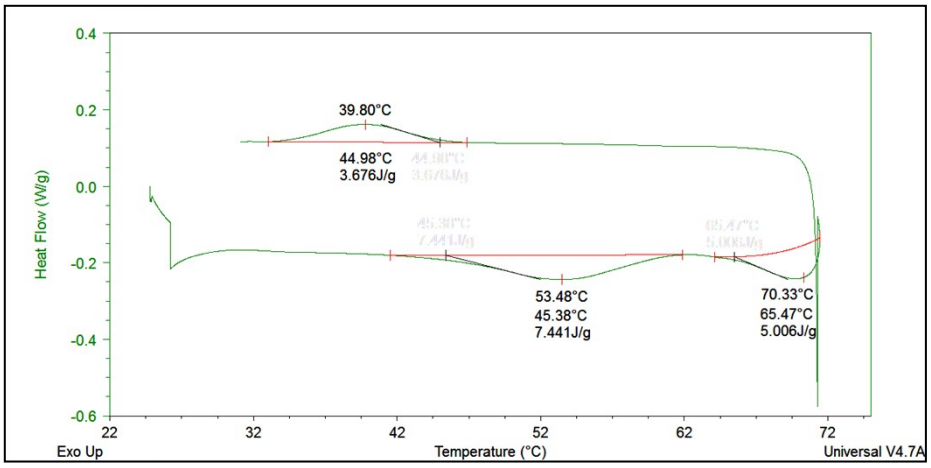

Figure S34. DSC curve of gel formed from **3** (R = $COCH_3$) in toluene at heating rate of 5 °C min^{-1}.

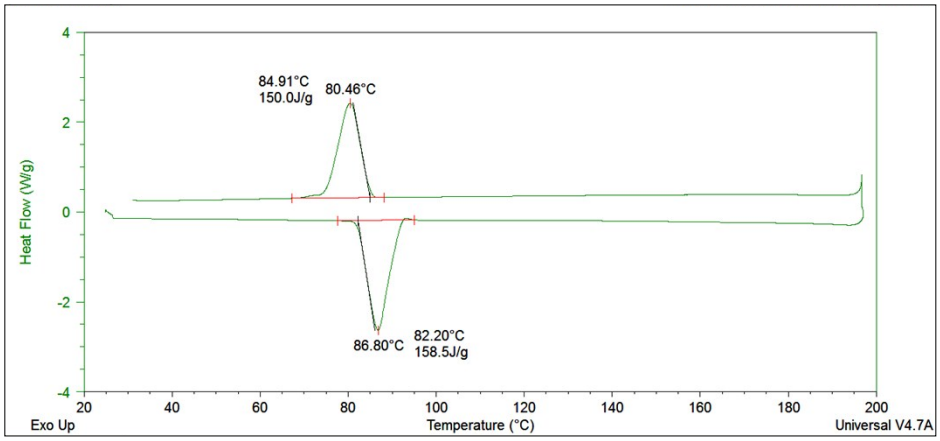

Figure S35. DSC curve for **1** (R = H) in powder form at heating rate of 5 °C min^{-1}.

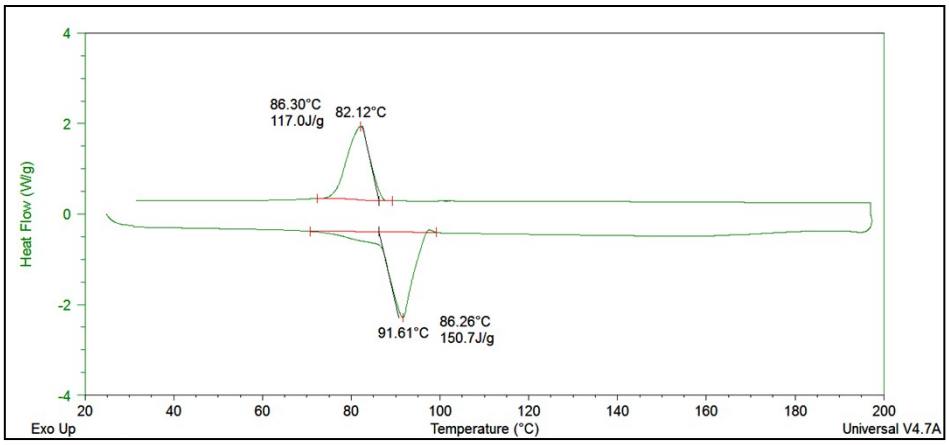

Figure S36. DSC curve for **2** (R = CH_3) in powder form at heating rate of 5 °C min^{-1}.

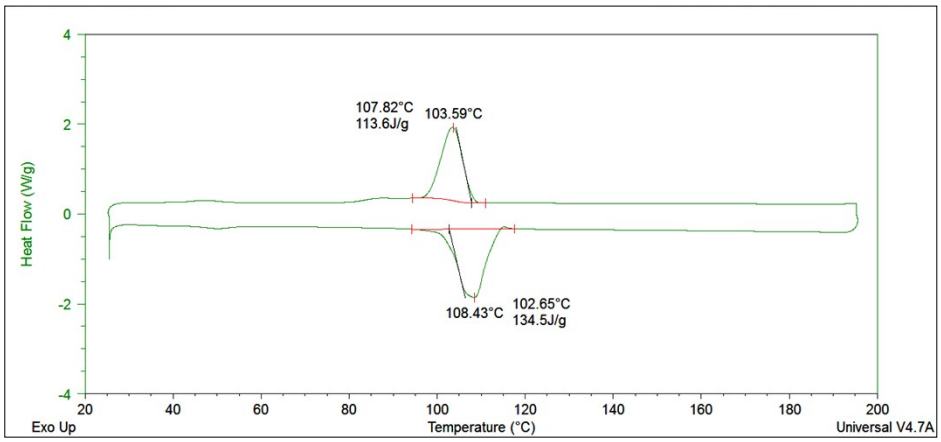

Figure S37. DSC curve for **3** (R = $COCH_3$) in powder form at heating rate of 5 °C min^{-1}.

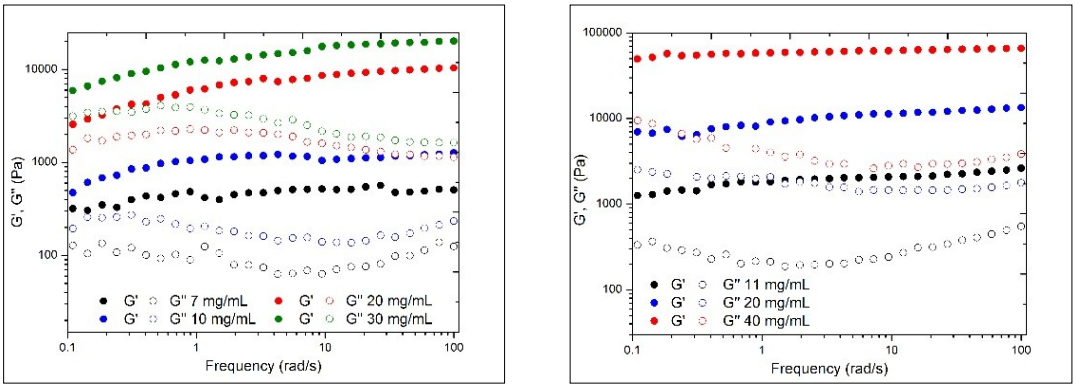

(a) (b)

Figure S38. Frequency sweeps (strain 0.02%) for gel of (a) **2** and (b) **3** formed in cyclohexane at different concentrations at 25 °C. G', Closed symbols and G'', open symbols.

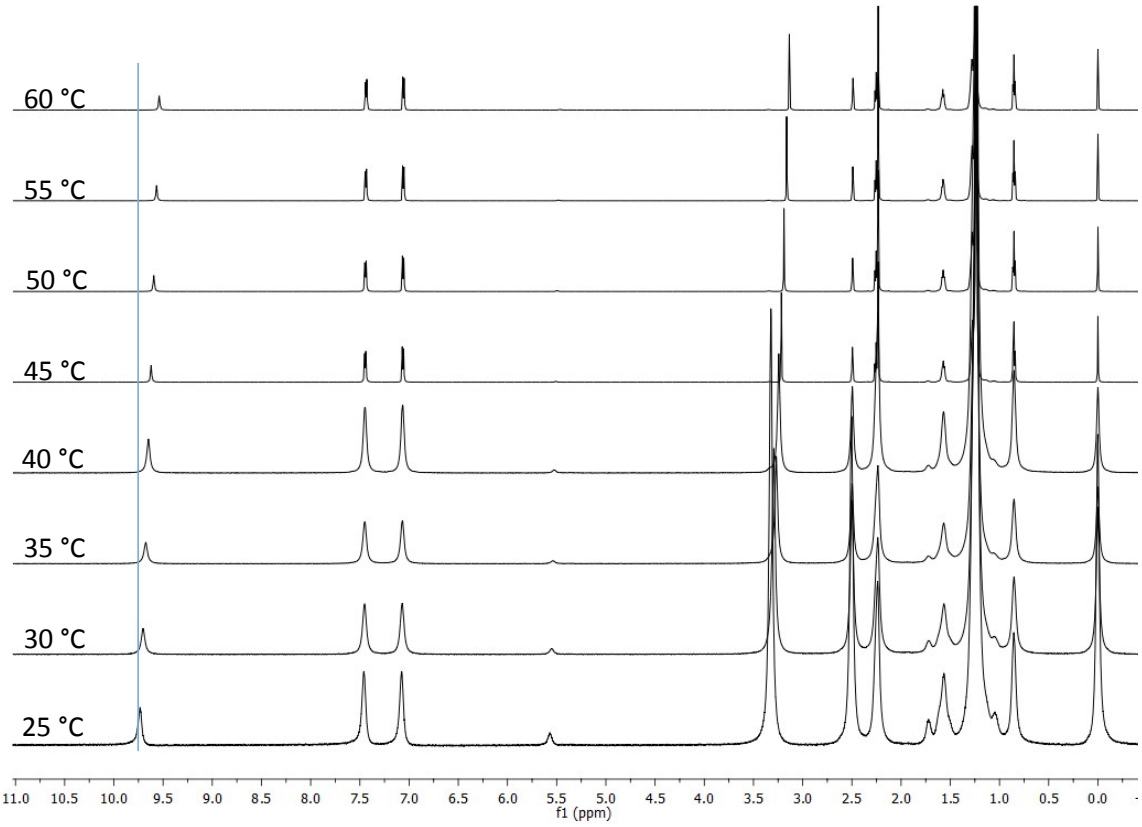

Figure S39. Superposition NMR ^{1}H spectra of compound **2** recorded in DMSO-d_6 solvent at different temperatures at concentration of 20 mg mL^{-1}.

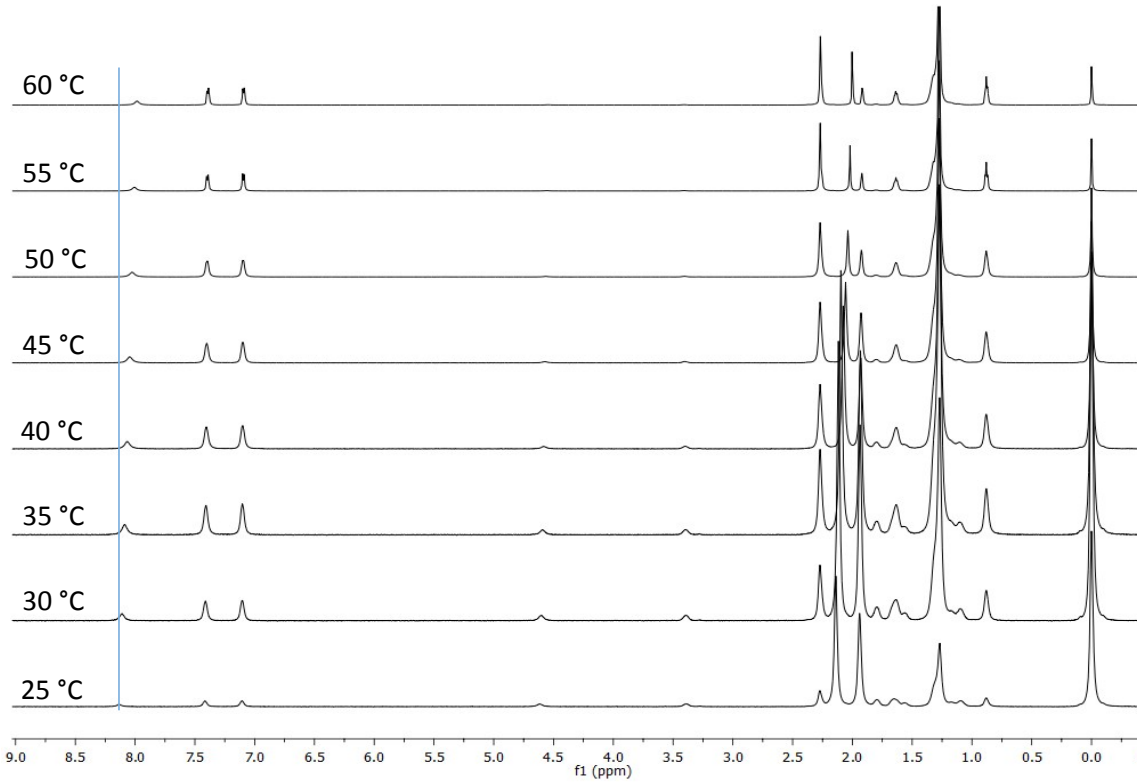

Figure S40. Superposition NMR ^{1}H spectra of compound **2** recorded in acetonitrile-d_3 solvent at different temperatures at concentration of 20 mg mL^{-1}.

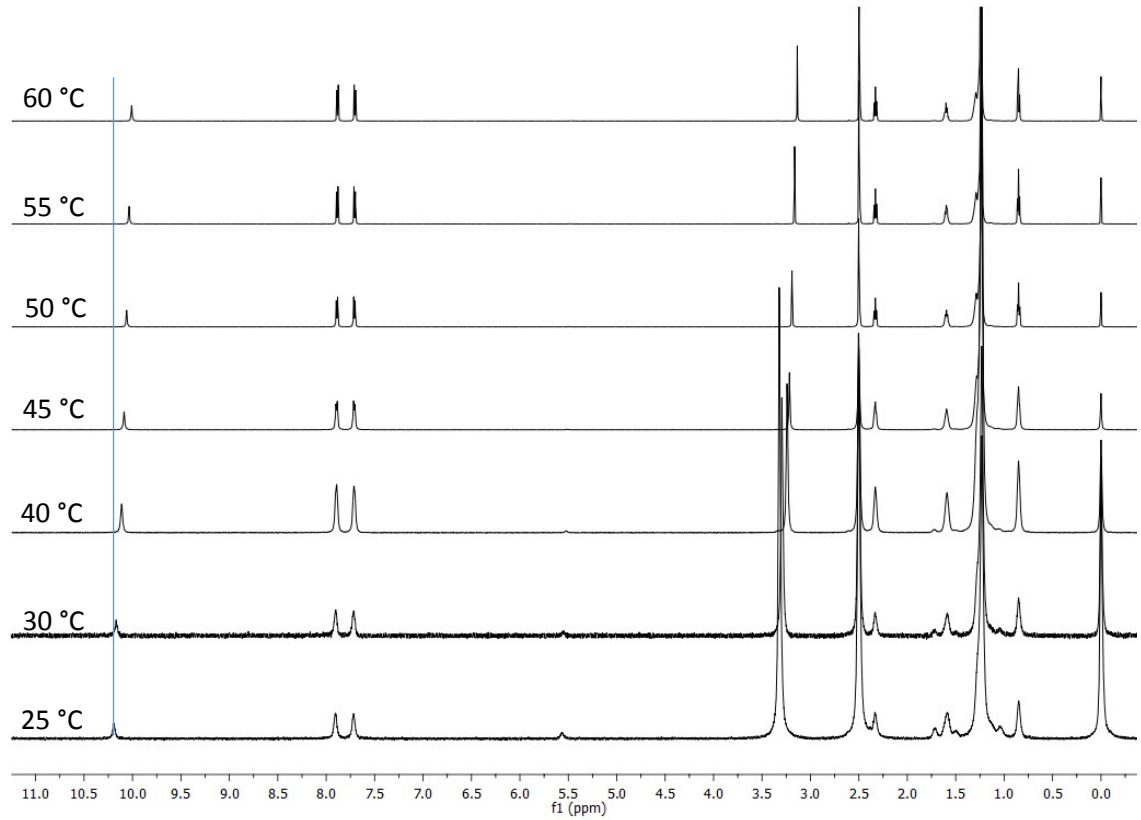

Figure S41. Superposition NMR ^{1}H spectra of compound **3** recorded in DMSO-d_6 solvent at different temperatures at concentration of 20 mg mL^{-1}.

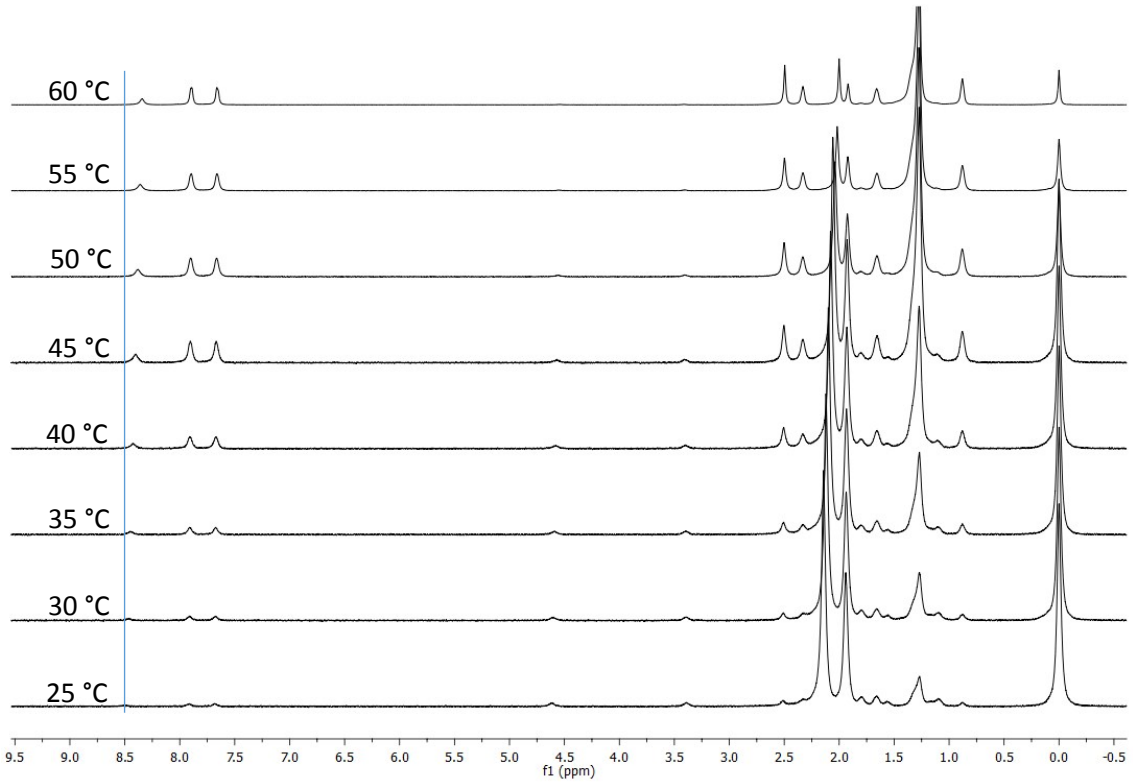

Figure S42. Superposition NMR ^{1}H spectra of compound **3** recorded in acetonitrile-d_3 solvent at different temperatures at concentration of 20 mg mL^{-1}.

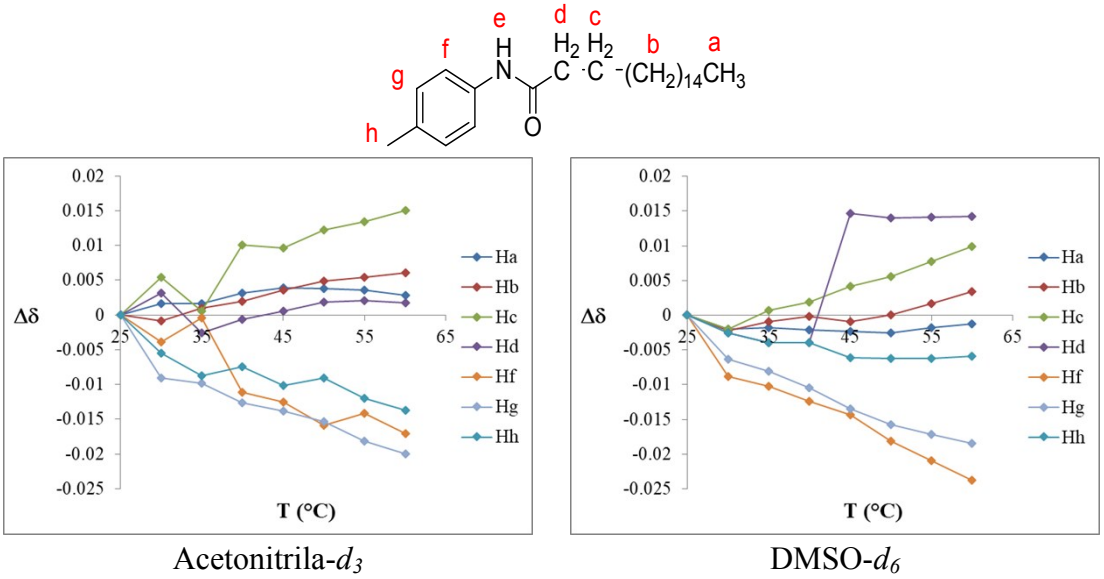

Acetonitrila-d_3 DMSO-d_6

Figure S43. ^{1}H NMR chemical shift changes of signals of compound **2** with temperature.

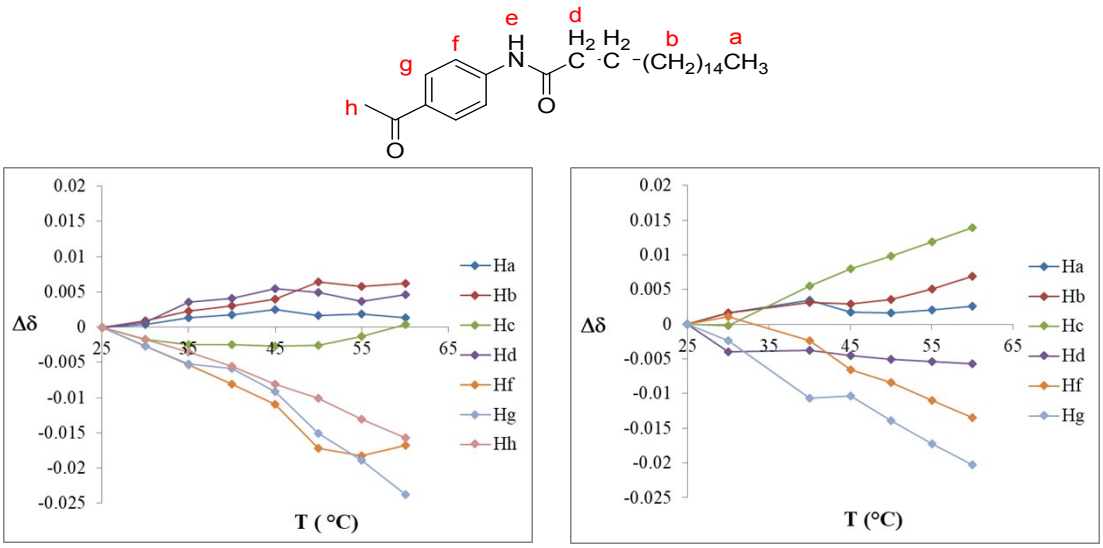

Acetonitrila-d_3 DMSO-d_6

Figure S44. ^{1}H NMR chemical shift changes of signals of compound **3** with temperature.

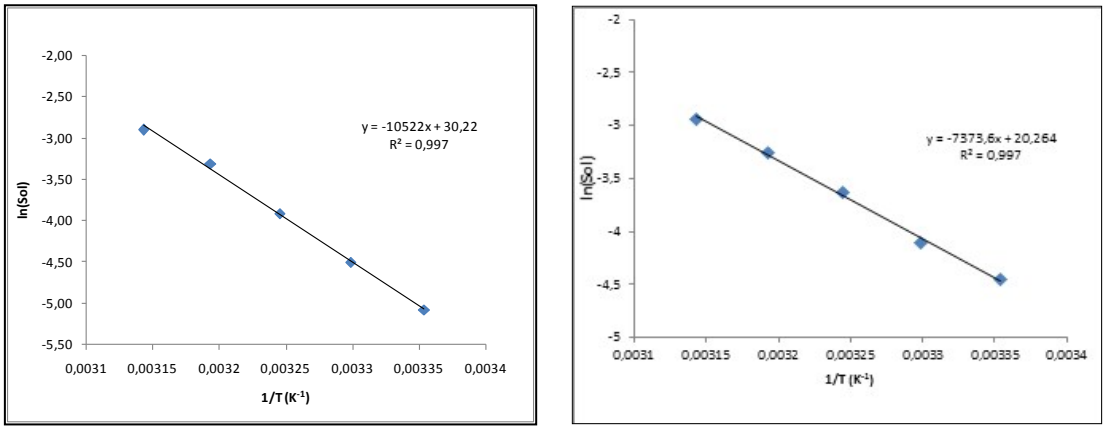

1 **2**

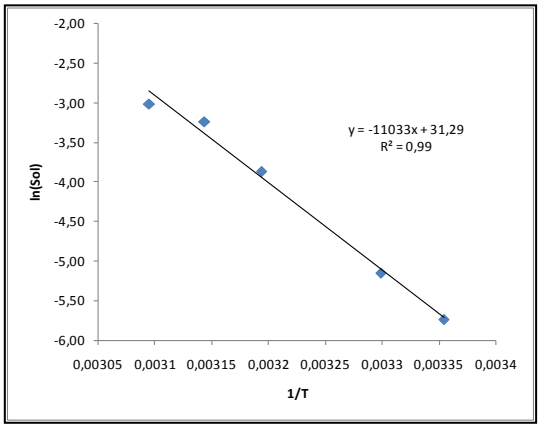

3

Figure S45. Plot of Ln(Sol) (Sol = solubility, i.e., the concentration of gelator molecules in solution) against the reciprocal of the dissolution temperature for compound **1-3** in DMSO-d_6.

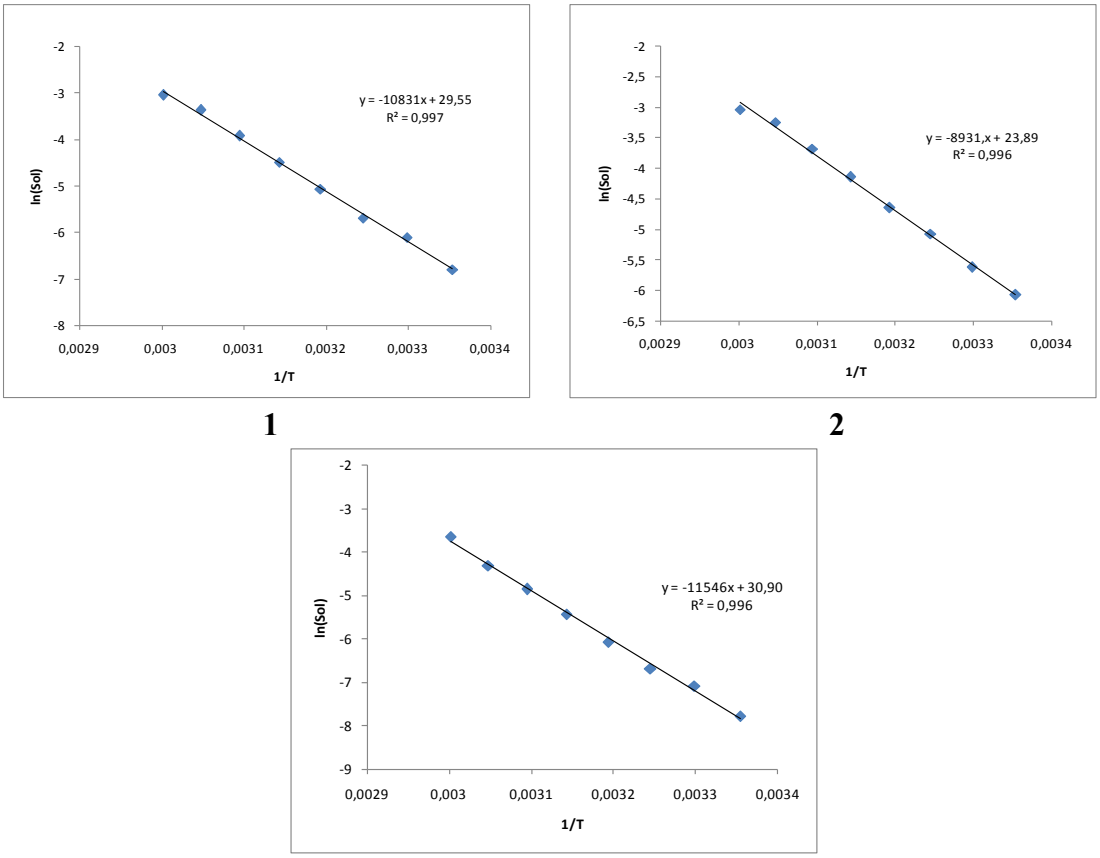

Figure S46. Plot of Ln(Sol) (Sol = solubility, i.e., the concentration of gelator molecules in solution) against the reciprocal of the dissolution temperature for compound **1-3** in acetonitrile-d_6.